Biochemical Pharmacology, Vol. 57, pp. 685–695, 1999.

ISSN 0006-2952/99/$–see front matter
PII S006-2952(98)00333-5

Inhibition of Oxidant-Induced Barrier Disruption and Protein Tyrosine Phosphorylation in Caco-2 Cell Monolayers by Epidermal Growth Factor

Radhakrishna Rao, Robert D. Baker and Susan S. Baker*

Division of Gastroenterology, Department of Pediatrics, Medical University of South Carolina, Charleston, SC 29425, U.S.A.

ABSTRACT. The effect of epidermal growth factor (EGF) on the H_2O_2-induced increase in paracellular permeability in Caco-2 and T-84 cell monolayers was evaluated to examine the role of EGF in intestinal mucosal protection from oxidative stress. Oxidative stress was induced by exposing cell monolayers to H_2O_2 or a mixture of xanthine oxidase + xanthine (XO + X). Paracellular permeability was assessed by measuring transepithelial electrical resistance (TER), sodium chloride dilution potential, and unidirectional flux of [^{3}H]mannitol. H_2O_2 (0.1 to 5.0 mM) reduced TER and dilution potential and increased mannitol flux. Administration of EGF delayed H_2O_2 and XO + X-induced changes in TER, dilution potential, and [^{3}H]mannitol flux. This protective effect of apically or basally administered EGF was concentration-related, with A_{50} (95% confidence limits) values of 2.1 (1.17 to 4.34) and 6.0 (4.37 to 8.34) nM, respectively. The EGF-mediated protection was prevented by treatment of cell monolayers with genistein (10 μM), a tyrosine kinase inhibitor. H_2O_2 and XO + X also induced tyrosine phosphorylation of a number of proteins in Caco-2 and T-84 cell monolayers. EGF treatment inhibited the oxidant-induced tyrosine phosphorylation of proteins, particularly those with a molecular mass of 110–220 kDa. Treatment of Caco-2 cells with anti-transforming growth factor-α antibodies potentiated the H_2O_2-induced changes in TER, dilution potential, and mannitol flux. These studies demonstrated that an EGF receptor-mediated mechanism delays oxidant-induced disruption of the epithelial barrier function, possibly by suppressing the oxidant-induced tyrosine phosphorylation of proteins. BIOCHEM PHARMACOL **57**;6:685–695, 1999. © 1999 Elsevier Science Inc.

KEY WORDS. epithelium; intestine; permeability; tyrosine kinase; tight junction; EGF

The intestinal epithelium *in vivo* is exposed to ROS† from multiple luminal and systemic sources. The potential sources of luminal ROS include xenobiotics, toxins, catalase-negative bacteria, mycoplasma, bile acids, and cast-off mucosal cells [1]. Systemic ROS are derived from mucosal inflammatory cells. Mucosal infiltration of polymorphonuclear neutrophils is common in inflammatory bowel disease and other intestinal disorders [2, 3]. Furthermore, neutrophils are present on the luminal side, especially in crypt abscesses found in Crohn's disease. The tissue level of H_2O_2 *in vivo* under physiologic or pathologic conditions is not known. An accurate assay of H_2O_2 *in vivo* is prevented by its rapid metabolism by antioxidant enzymes and quick conversion into other, more toxic, oxidant species. Vissers *et al.* [4], however, elegantly showed that neutrophils predominantly generate H_2O_2 at the site of adhesion, and the H_2O_2 concentration within the neutrophil-target cell cleft reaches 0.1 to 1.0 M.

In a recent study, we showed that H_2O_2 (0.5 to 10 mM) disrupts the paracellular junctions in Caco-2 and T-84 cell monolayers [5], with no significant effect on lactate dehydrogenase release [5]. Our study also showed that H_2O_2 increased tyrosine phosphorylation of a number of proteins in Caco-2 and T-84 cells, and that the H_2O_2-induced increase in paracellular permeability was mediated by a tyrosine kinase-dependent mechanism [5]. Oxidant-mediated epithelial injury plays an important role in the pathogenesis of intestinal inflammatory disorders, including inflammatory bowel disease [1–3]. Therefore, the factors that protect tissues from oxidant injury have clinical significance. Such an important mucosal protective factor in the gastrointestinal tract is EGF.

EGF, a single chain polypeptide [6], is released in various gastrointestinal secretions and regulates a number of gastrointestinal functions, suggesting that it has physiologic or pathophysiologic implications for the gastrointestinal system [7]. In addition to its growth-promoting activity, EGF also produces a number of acute effects in the gastrointestinal tract. Such an acute action of EGF is the protection of gastrointestinal mucosa from luminal irritants [8]. Both oral

* Corresponding author: R. K. Rao, Ph.D., Division of Gastroenterology, Department of Pediatrics, Medical University of South Carolina, 158 Rutledge Ave., Charleston, SC 29403. Tel. (843) 792-5039; FAX (843) 792-6472; E-mail: raor@musc.edu

† *Abbreviations*: ROS, reactive oxygen species; FBS, fetal bovine serum; EGF, epidermal growth factor; TGF-α, transforming growth factor-α; TER, transepithelial electrical resistance; PMSF, phenylmethylsulfonyl fluoride; and XO + X, xanthine oxidase + xanthine.

Received 20 February 1998; accepted 19 August 1998.

and systemic EGF proved to be cytoprotective in gastric ulceration induced by aspirin [9], stress [10, 11], ethanol [12, 13], and acid [14, 15], and duodenal ulceration induced by cysteamine [9, 16]. Additionally, recent studies demonstrated that EGF plays a protective role in the intestinal mucosa and cultured intestinal epithelium against various injurious factors [17–19]. In this study, we examined the protective effect of EGF in oxidant (5 mM H_2O_2 or XO + X)-induced intestinal epithelial-barrier disruption and protein tyrosine phosphorylation using the cultured monolayers of Caco-2 and T-84 cells. Caco-2 cells are known to express and secrete TGF-α [20, 21], and, therefore, we also investigated the possible presence of autocrine defense against oxidant injury using a mouse monoclonal anti-TGF-α antibody.

MATERIALS AND METHODS

Cell Culture

Caco-2 cells, originally obtained from Dr. Jeffrey Field, were maintained under standard cell culture conditions at 37° in Dulbecco's modified Eagle's medium (DMEM) containing 20% (v/v) FBS. Cells were grown on polycarbonate membranes in Transwells (6.5 mm; Costar). Experiments were performed on day 12 or 13 after seeding cells onto Transwells (within passages No. 40–55). Under these conditions, confluent monolayers attained steady-state resistance to passive transepithelial ion flow, and neighboring cells were adjoined by circumferential intercellular tight junctions that restrict the passive flow of ions and solutes as described previously [22, 23]. T-84 cells (American Type Culture Collection) were grown similarly in a mixture (1:1) of DMEM and Ham's F12 nutrient mixture containing 6% FBS, HEPES (15 mM), and antibiotics (penicillin, ampicillin, and streptomycin).

Oxidant and Other Treatments

Monolayers were bathed in PBS/BSA (Dulbecco's saline containing 1.2 mM $CaCl_2$, 1 mM $MgCl_2$, and 0.6% BSA), 0.2 mL and 1.0 mL applied to apical and basal wells, respectively. After 1 hr equilibration in PBS/BSA, H_2O_2 was administered to the apical or basal medium in 10-μL aliquots to achieve a final concentration of 0.1 to 5.0 mM. In some experiments, a mixture of xanthine oxidase (20 mU/mL) and xanthine (0.25 mM) (XO + X) was administered to the apical and basal media. EGF was administered to the apical or basal medium 60 min prior to H_2O_2 (unless mentioned otherwise) to achieve different concentrations (1, 3, 10, or 30 nM). EGF, once administered, was retained in the medium until the end of the experiment (unless mentioned otherwise). In some experiments, genistein (10 μM) was administered to the apical and the basal media 10 min prior to EGF administration.

Calcium depletion was developed by omitting calcium chloride from PBS/BSA. An osmotic gradient was induced by including 0.5 M mannitol in the apical medium. Mouse monoclonal anti-TGF-α antibodies or pre-immune mouse IgG were administered to both apical and basal media 30–120 min prior to H_2O_2 administration followed by the continuous presence during oxidant treatment.

Measurement of TER

TER was measured according to the method of Hidalgo *et al.* [22] using a Millicell-ERS Electrical Resistance System (Millipore) and calculated as $\Omega \cdot cm^2$ by multiplying it with the surface area of the monolayer (0.33 cm^2. The resistance of the supporting membrane in Transwells (which is usually around 30 $\Omega \cdot cm^2$) was subtracted from all readings prior to calculations.

Unidirectional Flux of [^{3}H]Mannitol

Cell monolayers in Transwells were incubated under different experimental conditions in the presence of 0.2 μCi/mL of D-[2-^{3}H]mannitol (15 Ci/mmol; ICN Biomedicals, Inc.) in the basal medium. At different times after H_2O_2 administration, 100 μL each of apical and basal media were withdrawn, and radioactivity was counted in a scintillation counter (Beckman LS 3801). The flux into the apical medium was calculated as the percent of total isotope administered into the basal well per hour per cm^2 surface area.

Measurement of Dilution Potential

Twenty percent sodium chloride dilution potential was measured as previously described by Madara *et al.* [24]. At the end of experimental treatments, monolayers were washed once with PBS/BSA and bathed in fresh PBS/BSA, 0.2 and 1.0 mL to apical and basal compartments, respectively. Transepithelial potential difference was recorded using the Millicell-ERS Electrical Resistance System. Twenty percent sodium chloride dilution in the apical medium was developed by replacing 40 μL of apical medium with 40 μL of PBS/BSA in which sodium chloride was replaced with equi-osmolar mannitol. Potential difference was recorded again, and the difference between the initial potential difference and the potential difference recorded after 20% dilution was calculated as dilution potential (mV).

Protein Tyrosine Phosphorylation

Immediately after the experimental treatment, monolayers were washed with 2 mL of cold PBS without BSA. Then the cell monolayer was lysed in 100 μL of hot lysis buffer (0.05 M Tris, pH 8.0, containing 1% SDS, 0.1 mM vanadate, and 0.1 mM PMSF). Cell lysate was then heated at 100° for 5 min and homogenized by passing through a 28-gauge needle 10 times. The homogenate was centrifuged at 5000 *g* for 10 min, and the supernatant was used for

western blotting. Protein content of the supernatants was analyzed by the BCA method (Pierce).

Proteins were separated by SDS–PAGE on 7.5% gel and transferred to nitrocellulose (PVDF) membranes. Phosphotyrosyl proteins were detected by blotting with anti-phosphotyrosine antibodies conjugated with horseradish peroxidase and staining with the enhanced chemiluminescence method.

Densitometric Analysis of Western Blots

Autofluorograms were scanned using an Imaging Densitometer (BIORAD GS-670). The volume of the optical density of different bands was analyzed by selecting a constant area (at specific molecular mass range) using the computer software "Molecular Analyst." Local area background O.D. was subtracted from each band and volume was calculated as O.D. · mm^2. Quantitation was compared within the samples and controls in a single blot.

Chemicals

Cell culture media and related reagents were purchased from GIBCO-BRL, while genistein was from Calbiochem. EGF, pre-immune mouse IgG, and all other chemicals were of analytical grade, and were purchased from the Sigma Chemical Co. Mouse monoclonal anti-TGF-α antibody was purchased from Oncogene Science. Mouse monoclonal anti-phosphotyrosine-HRP antibodies were from Transduction Laboratories, and the enhanced chemiluminescence peroxidase staining kit was from the Amersham Corp.

Statistics

Comparison between two groups was made by Student's *t*-tests for grouped data or by analysis of variance and Fisher's *post hoc* test for comparisons of more than two groups. Significance in all tests was derived at the 95% or greater confidence level.

RESULTS

Paracellular Permeability in Caco-2 Cell Monolayer

Baseline TER of Caco-2 cell monolayers (12- or 13-day post-seeding) varied from 300 to 450 Ω · cm^2. Administration of H_2O_2 to the basal surface at final concentrations of 0.1 to 5.0 mM reduced the TER in a time- and concentration-related manner (Fig. 1). Administration of EGF (30 nM) to the apical or basal buffer by itself produced no significant effect on baseline TER. However, EGF administered 60 min prior to H_2O_2 (5 mM) significantly inhibited the H_2O_2-induced decrease in TER (Fig. 2A). EGF was equally effective in inhibiting H_2O_2-induced decrease in TER when administered to either apical or basal surface of cell monolayers. This epithelial protective effect of EGF was concentration-related with A_{50} (95% confidence limits) values of 2.1 (1.17 to 4.34) and 6.0 (4.37 to 8.34) nM

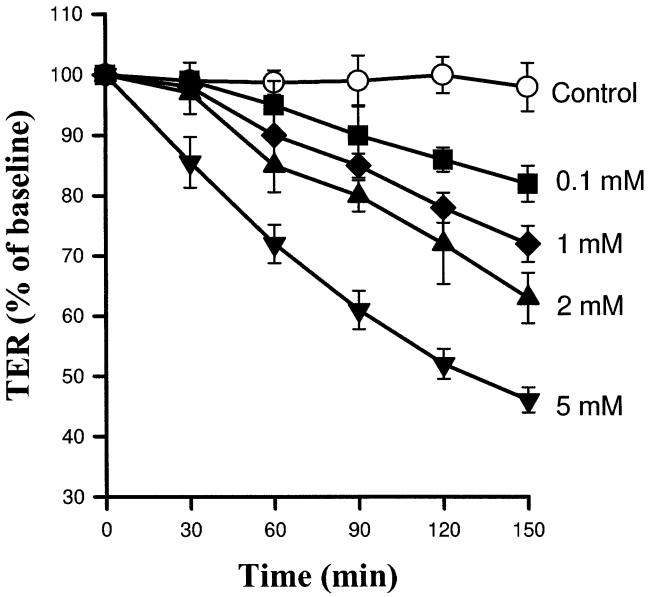

FIG. 1. Time- and concentration-related decrease in TER caused by H_2O_2. Caco-2 cell monolayers were treated with 0.1 to 5.0 mM H_2O_2 at the basal surface, and TER was monitored at different times. Values are means ± SEM (N = 5 for each group). The baseline TER values varied from 238 ± 23 to 295 ± 25 3 Ω · cm^2.

for apical and basal administration, respectively (Fig. 2B). Administration of H_2O_2 also reduced the sodium chloride dilution potential of Caco-2 cell monolayers in a time-dependent manner with a significant reduction achieved at 60 min (Fig. 3A). H_2O_2-induced reduction of dilution potential was inhibited significantly by both apical and basal EGF treatment (Fig. 3A); EGF alone produced no significant effect on baseline dilution potential. Unidirectional flux of [^{3}H]mannitol was negligibly low in control monolayers, and it was not altered during a 150-min incubation in PBS/BSA. Administration of H_2O_2 increased the unidirectional flux of [^{3}H]mannitol by 4-fold at 120 min and 9-fold at 150 min (Fig. 3B). This H_2O_2-induced increase in [^{3}H]mannitol flux was prevented by treatment with EGF (30 nM) at the apical or basal surface. EGF by itself produced no significant effect on mannitol flux.

EGF (apical or basal) administration significantly reduced H_2O_2-induced decrease in TER also when EGF was present for only 60 min prior to the H_2O_2 administration (Fig. 4A) or when it was introduced 30 min after H_2O_2 administration (Fig. 4B). However, these effects were weaker than the effect when EGF was present throughout the experiment (Fig. 2A). Calcium depletion or osmotic gradient induced a reduction in TER of Caco-2 cell monolayers (Fig. 4C). Treatment of monolayers with apical or basal EGF (30 nM) failed to affect the reduction of TER induced by calcium depletion or osmotic gradient (Fig. 4C). Treatment of Caco-2 cell monolayers with genistein (10 μM), an inhibitor of tyrosine kinases, produced no significant effect on baseline TER of control monolayers (Fig. 5). Genistein (10 μM) also failed to affect the H_2O_2-induced

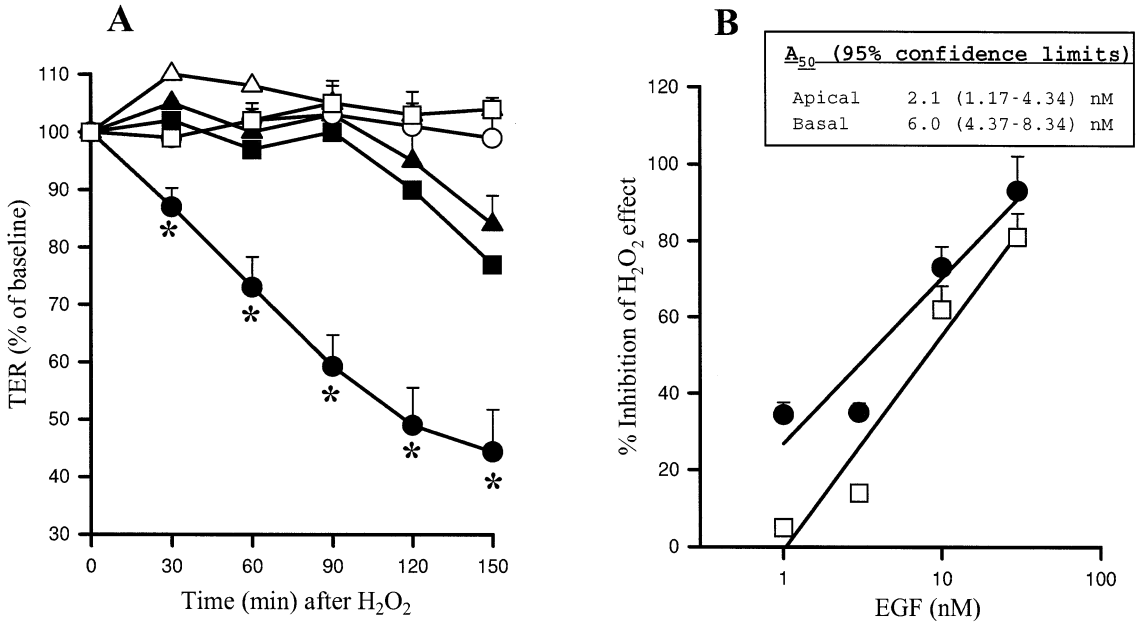

FIG. 2. (A) Time course of the effect of 5 mM H_2O_2 on TER of Caco-2 cell monolayers (●) and monolayers that were pretreated with 30 nM apical (▲) or basal (■) EGF. Open symbols represent control monolayers without (○) or with apical (△) or basal (□) EGF. Monolayers in Transwells were bathed in PBS/BSA, and EGF was applied 60 min prior to the administration of H_2O_2. Values are means ± SEM (N = 6 for each group). The baseline TER values varied from 249 ± 13 to 285 ± 10 3 Ω · cm^2. Asterisks indicate values that were significantly different ($P < 0.05$) from corresponding values for H_2O_2 in EGF-treated monolayers. (B) Non-cumulative concentration–effect curves for apical (●) and basal (□) EGF-mediated inhibition of H_2O_2-induced decrease in TER in Caco-2 monolayers. Monolayers in Transwells were bathed in PBS/BSA, and EGF (1–30 nM, apical or basal) was applied 60 min prior to the administration of H_2O_2. Decreases in TER were assessed at 120 min after H_2O_2 administration. Values are means ± SEM (N = 6 for each group). The inset table presents the EGF concentration that produced 50% inhibition of H_2O_2-induced decrease in TER.

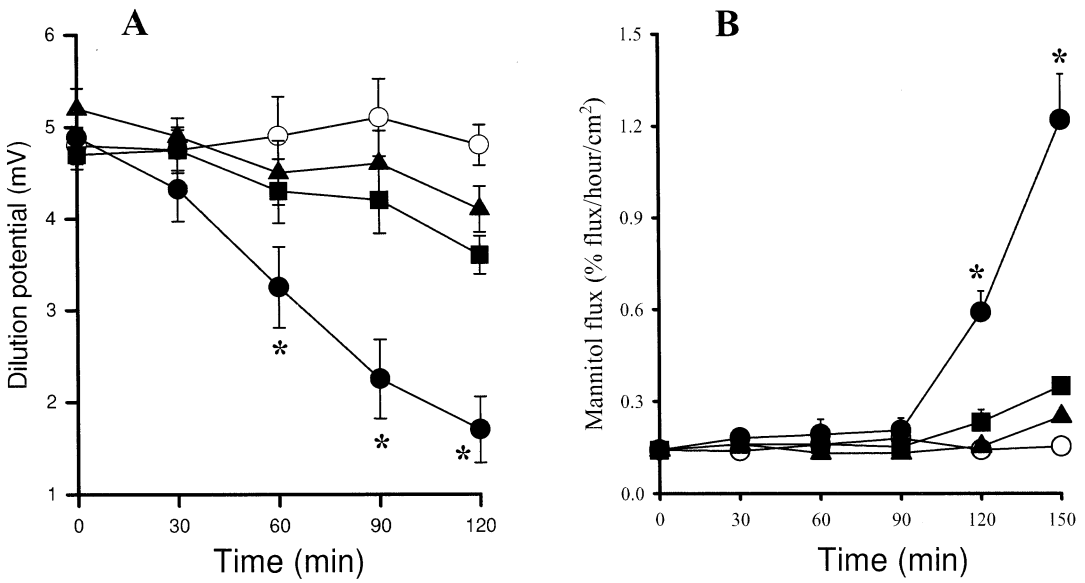

FIG. 3. Effect of EGF (30 nM) on H_2O_2-induced decrease in dilution potential (A) and mannitol flux (B) measured at various times after H_2O_2 (5 mM) administration without (●) or with EGF at the apical (A-EGF; ▲) or the basal (B-EGF; ■) surface administered 60 min prior to H_2O_2. Control monolayers (○) received no H_2O_2 or EGF. Values are means ± SEM (N = 6 for each group). Asterisks indicate values for the H_2O_2 group that were significantly different ($P < 0.05$) from corresponding values for the control or the H_2O_2 + EGF group.

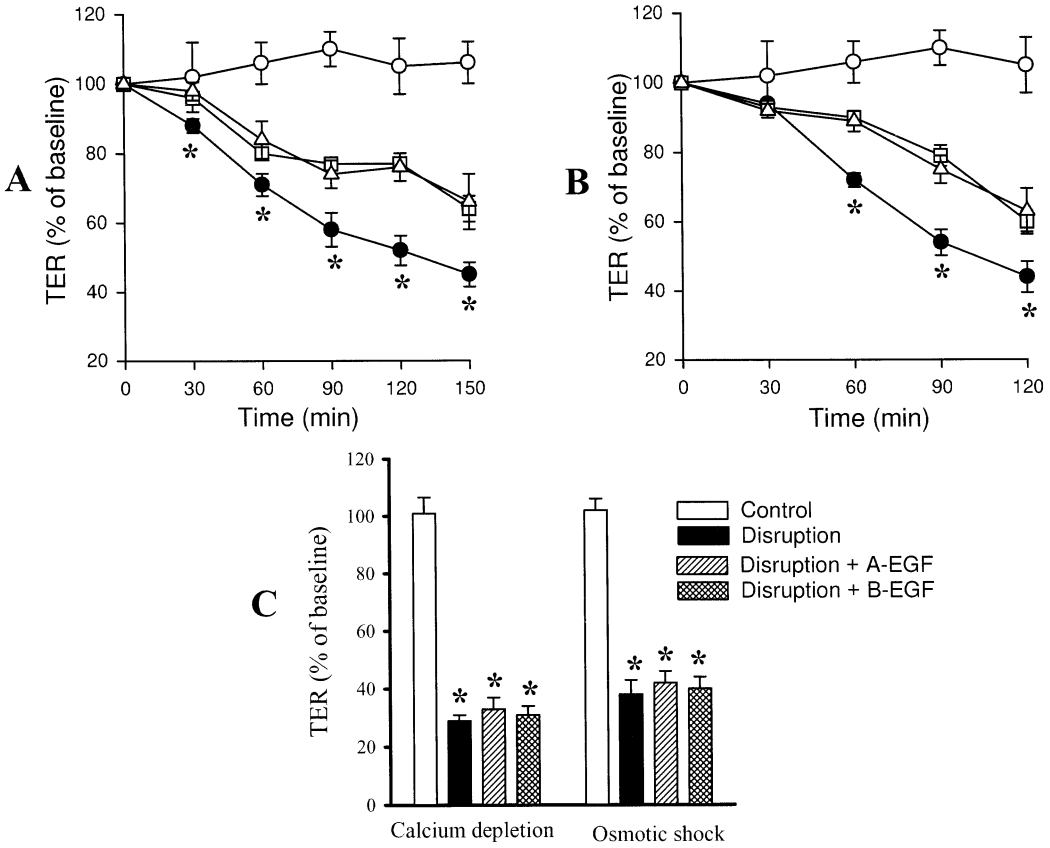

FIG. 4. (A) Effect of EGF on H_2O_2-induced decrease in TER of Caco-2 cell monolayers. Cell monolayers were incubated with saline (●) or EGF (30 nM) at the apical (△) or basal (□) surface for 60 min prior to H_2O_2 (5 mM) administration. Control (○) monolayers received no H_2O_2. Values are means ± SEM (N = 6 for each group). Asterisks indicate values for the H_2O_2 group (●) that were significantly ($P < 0.05$) different from corresponding values for EGF-treated monolayers. (B) This experiment is identical to A, except that EGF was applied 30 min after H_2O_2 administration. (C) Effect of EGF (30 nM) on the reduction of TER in Caco-2 cell monolayers induced by calcium depletion (calcium-free medium containing 0.1 mM EGTA) or osmotic gradient (0.5 M mannitol in apical buffer). Controls received no EGF, nor were they subjected to osmotic gradient or calcium depletion. The decrease in TER was assessed at 60 min after calcium depletion or mannitol administration. Values are means ± SEM (N = 6 for each group). Asterisks indicate values that were significantly ($P < 0.05$) different from control values.

reduction of TER. However, treatment with genistein (10 μM) applied 10 min prior to EGF administration almost completely prevented EGF-mediated suppression of H_2O_2-induced reduction of TER.

Protein Tyrosine Phosphorylation in Caco-2 Cell Monolayer

Western blot analysis detected no tyrosine-phosphorylated proteins in the extracts of untreated Caco-2 cell monolayers under the present experimental conditions. However, administration of H_2O_2 resulted in tyrosine phosphorylation of a number of proteins in a concentration-related manner (Fig. 6A). Protein clusters with a molecular mass of 50–90 kDa and 110–170 kDa were the prominent tyrosine-phosphorylated proteins. Treatment of monolayers with EGF at the apical or basal surface inhibited H_2O_2-induced protein tyrosine phosphorylation in a concentration-related manner (Fig. 6B). Tyrosine phosphorylation of a cluster of proteins with a molecular mass of 110–170 kDa was strongly inhibited by EGF administration (Fig. 6C); phosphorylation of proteins with a molecular mass of 180–220 kDa was also inhibited to some extent. However, tyrosine phosphorylation of proteins at the molecular mass range of 60–85 kDa was unaffected by apical EGF, or showed minimal inhibition by basal EGF.

XO + X-Induced Increase in Paracellular Permeability and Protein Tyrosine Phosphorylation in T-84 Cell Monolayers

Treatment of T-84 cell monolayers with XO + X also reduced TER (Fig. 7A) and dilution potential (Fig. 7B) and increased mannitol flux (Fig. 7C). EGF (10 nM) administration significantly reduced the XO+X-induced changes in TER and mannitol flux in this epithelium (Fig. 7). XO + X treatment also induced tyrosine phosphorylation of a wide spectrum of proteins in T-84 cell monolayer (Fig. 8A). EGF administration prevented the XO+X-induced tyrosine phosphorylation of proteins with a molecular mass of 110–170 kDa and 180–220 kDa, while tyrosine phos-

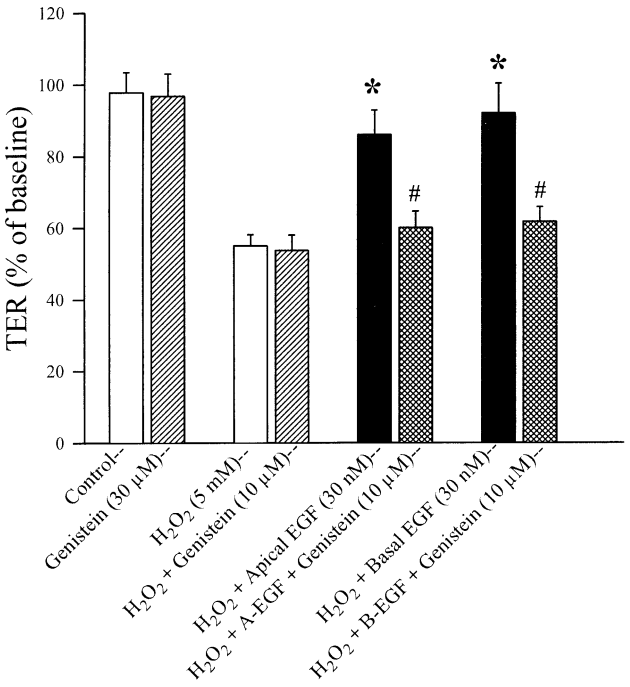

FIG. 5. Effect of EGF, apical (A-EGF) or basal (B-EGF), on H_2O_2-induced decrease in TER in Caco-2 monolayers: Inhibition by genistein. TER was assessed at 90 min after H_2O_2 administration. Values are means ± SEM (N = 6 for each group). Key: (*) and (#) indicate values that were significantly different ($P < 0.05$) from values for the H_2O_2 alone group or the H_2O_2 + EGF group, respectively.

phorylation of proteins with a molecular mass of 60–85 kDa was unaffected (Fig. 8B).

Protection by Endogenous TGF-α

Caco-2 cell monolayers are known to express TGF-α [23, 24], an EGF-like peptide that activates EGF receptors [7]. Treatment of cell monolayers with anti-TGF-α antibodies (1 μg/mL) significantly potentiated the H_2O_2-induced decrease in TER (Fig. 9A), whereas treatment with preimmune mouse IgG (1 μg/mL) produced no effect (data not shown). Anti-TGF-α antibody also potentiated the effect of H_2O_2 on dilution potential (Fig. 9B) and mannitol flux (Fig. 9C). Anti-TGF-α antibody at a concentration of 100 ng/mL produced maximal potentiation of H_2O_2-induced decrease in TER (Fig. 10A) and increases in mannitol flux (Fig. 10B). Administration of anti-TGF-α antibody 30 min prior to H_2O_2 exposure was sufficient to produce a potentiation of H_2O_2-induced changes in TER and mannitol flux. Presence of EGF (30 nM) at the apical or basal surfaces prevented the potentiation of H_2O_2-induced changes in TER (Fig. 11A), dilution potential (Fig. 11B), and mannitol flux (Fig. 11C) by anti-TGF-α antibody.

DISCUSSION

The present study demonstrated that EGF delays oxidant-induced increase in paracellular permeability in Caco-2 and T-84 cell monolayers. Exposure to H_2O_2 (0.1 to 5.0 mM) reduced the TER of Caco-2 cell monolayers in a time- and concentration-related manner. This effect of H_2O_2 was associated with a decrease in sodium chloride dilution potential and an increase in unidirectional flux of [^{3}H]mannitol. As described above, the concentration of H_2O_2 used is well within the pathophysiologic concentration range, indicating the clinical relevance of this response. A decrease in dilution potential indicates a reduction in charge selectivity of the tight junctions. The tight junctions of the intestinal epithelium impede the movement of anions, while cations readily diffuse through [22]. The increase in mannitol flux is an indicator of a disruption of the structure of tight junctions and an increase in paracellular permeability to macromolecules. Treatment of monolayers with EGF significantly delayed these H_2O_2-induced changes in TER, dilution potential, and mannitol flux, suggesting that EGF may have a protective effect on the intestinal epithelium in oxidant-induced epithelial injury. Results showed that a similar EGF-induced epithelial protection could be demonstrated in T-84 cell monolayers. Both Caco-2 and T-84 cells are colon adenocarcinoma cell lines. While Caco-2 cells differentiate into villus-like cells, T-84 cells are a terminally differentiated chloride-secreting cell line. Both cell monolayers have been used extensively as models of intestinal epithelium for barrier function studies.

Under normal physiologic conditions, the intestinal epithelium is protected from injurious substances by various mucosal defense mechanisms. EGF is an important mediator of mucosal defense in the gastrointestinal tract, and it has been consistently shown to protect the gastrointestinal mucosa from damage by various luminal irritants [16–19]. Results of the present study show that EGF protects the Caco-2 and T-84 epithelia from the oxidant-induced disruption of paracellular junctions. The effect of EGF on epithelial permeability was rapid, as EGF application at 15 min prior to H_2O_2 was sufficient to produce its maximal effect. Low A_{50} values (2–6 nM) of EGF for the inhibition of H_2O_2-induced decrease in TER indicate that EGF is highly potent in producing this epithelial protective effect, with a significant inhibition achieved at 1 nM. The K_d value for binding of EGF to its receptors in a variety of cells has been shown to be 0.5 to 1.0 nM [7, 25], and the salivary EGF concentration in different species varies from 10 to 1000 nM [26]. Therefore, the observed high potency of EGF in protecting the epithelium from H_2O_2 indicates that this function of EGF may have a physiologic or pathophysiologic implication for the gastrointestinal epithelium.

The present study also shows that EGF protected Caco-2 cell monolayers from H_2O_2 when it was administered to either the apical or basal surface of the epithelium. This is supported by previous reports that EGF-specific receptors are present on both apical and basal surfaces of Caco-2 cell monolayers [25]. EGF receptors on both apical and basal surfaces of Caco-2 cells showed similar K_d values for EGF [25], and in the present study, apical EGF showed a potency similar to that of basal EGF. Previous studies have demon-

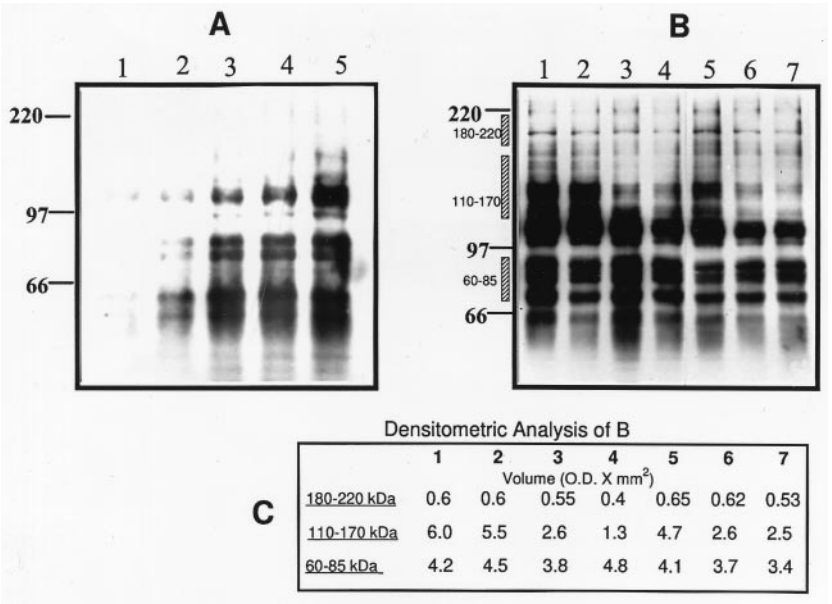

FIG. 6. H_2O_2-induced protein tyrosine phosphorylation in Caco-2 cell monolayers. (A) Protein tyrosine phosphorylation induced by 0.1 mM (lane 1), 0.5 mM (lane 2), 1.0 mM (lane 3), 2.0 mM (lane 4), and 5.0 mM (lane 5) H_2O_2. Caco-2 cell monolayers were exposed to various concentrations of H_2O_2 for 30 min. Extracted proteins (10 μg) were subjected to western blot analysis of phosphotyrosine using HRP-conjugated anti-phosphotyrosine antibody. Mobility of standard proteins is marked on the left-hand side of the blot; numbers indicate the molecular mass (kDa). (B) Effect of apical or basal EGF on H_2O_2-induced protein tyrosine phosphorylation. Caco-2 cell monolayers were exposed to 5 mM H_2O_2 at the basal surface for 30 min. Various concentrations of EGF were administered to the apical or the basal surface 30 min prior to H_2O_2. Proteins (10 μg) extracted 30 min after H_2O_2 were subjected to western blot analysis of phosphotyrosine using HRP-conjugated anti-phosphotyrosine antibody. Lane 1: 5 mM H_2O_2; lane 2: 1 nM apical EGF + H_2O_2; lane 3: 10 nM apical EGF + H_2O_2; lane 4: 30 nM apical EGF + H_2O_2; lane 5: 1 nM basal EGF + H_2O_2; lane 6: 10 nM basal EGF + H_2O_2; and lane 7: 30 nM basal EGF + H_2O_2. Control monolayers or monolayers treated with only EGF showed no detectable phosphotyrosine bands. Bars on the left margin represent different sets of bands selected for densitometric analysis (C). This experiment was repeated with similar results two other times.

strated that EGF is released in various gastrointestinal secretions at high concentrations and is under neurohormonal regulation [26]. The protective effect of apical EGF in Caco-2 cell monolayers suggests that luminally released EGF may modulate the intestinal epithelium by binding to the apical surface. However, extrapolation of such EGF activity at the apical surface of Caco-2 cell monolayers to the animal intestine is complicated by the failure to localize EGF specific receptors on the apical membranes of enterocytes [27, 28]. Although it has been demonstrated repeatedly that luminal EGF is biologically active, the mechanism involved in the activity of luminal EGF is not clear. A recent study demonstrated that luminal EGF protects the intestinal mucosa from fatty acid-induced injury by stimulating mucus secretion [17], which appears to involve a transepithelial translocation of EGF to the basal compartment, possibly at the injured epithelium. Therefore, it remains to be established if luminal EGF plays a physiologic role in the intact epithelium.

The epithelial protective effect of EGF was evaluated further in other models of epithelial paracellular junctional disruption. Calcium depletion and osmotic gradient (0.5 M mannitol at the apical surface) reduced TER of Caco-2 cell monolayers. EGF administration failed to affect these decreases in TER caused by calcium depletion and osmotic gradient. These results suggest that the observed epithelial protective effect of EGF may be specific to oxidant-induced increases in paracellular permeability.

Disruption of epithelial barrier function by ROS, especially H_2O_2, has been demonstrated in alveolar, breast, lens, and renal epithelial cells [29–34]. However, the mechanisms involved in the oxidant-induced increase in paracellular permeability are not known. We recently demonstrated that H_2O_2 increases paracellular permeability in Caco-2 cell monolayers by a tyrosine kinase-dependent mechanism [5]. We showed that vanadate, a phosphotyrosine phosphatase (PTPase) inhibitor, potentiated the H_2O_2-induced increase in paracellular permeability and protein tyrosine phosphorylation, while tyrosine kinase inhibitors such as genistein and tyrphostin inhibited the H_2O_2-induced increase in permeability and phosphorylation. The results of the present study show that EGF inhibits the H_2O_2-induced increase in tyrosine phosphorylation of a cluster of proteins with a molecular mass of 110–220 kDa. Similarly, EGF also inhibited XO + X-induced tyrosine phosphorylation of proteins, especially those with a molecular mass of 110–220 kDa, in T-84 cell monolayers. These results suggest that proteins of 110–220 kDa may play an important role in the maintenance of paracellular barrier function.

The intrinsic tyrosine kinase activity of the EGF receptor plays an important role in the mechanism of EGF action

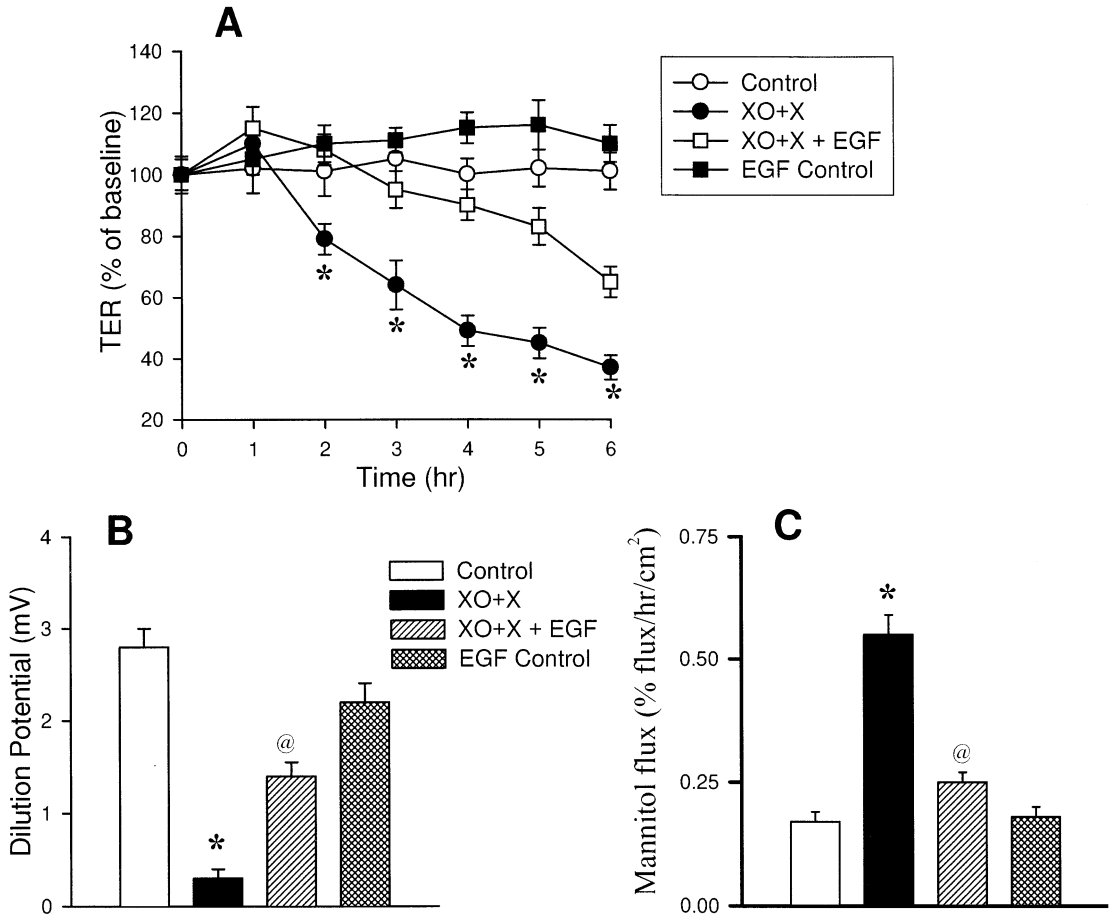

FIG. 7. (A) Effect of XO+X (●) or XO+X + EGF (10 nM) (□) on TER of T-84 cell monolayers at various times after XO+X administration. Control monolayers without (○) or with EGF (■) received no XO+X. EGF (60 min prior to XO+X) and XO+X were administered to both apical and basal compartments. Values are means ± SEM (N = 4). Asterisks indicate values that were significantly ($P < 0.05$) different from corresponding values for EGF + XO+X monolayers. (B and C) Effect of XO+X (closed) or EGF + XO+X (hatched) on dilution potential (B) and mannitol flux (C) in T-84 cell monolayers measured at 4 hr after XO+X administration. Control monolayers without (open) or with EGF (cross-hatched) received no XO+X. Values are means ± SEM (N = 4). Key: (*) and (@) indicate values that were significantly ($P < 0.05$) different from values for control and XO+X monolayers, respectively.

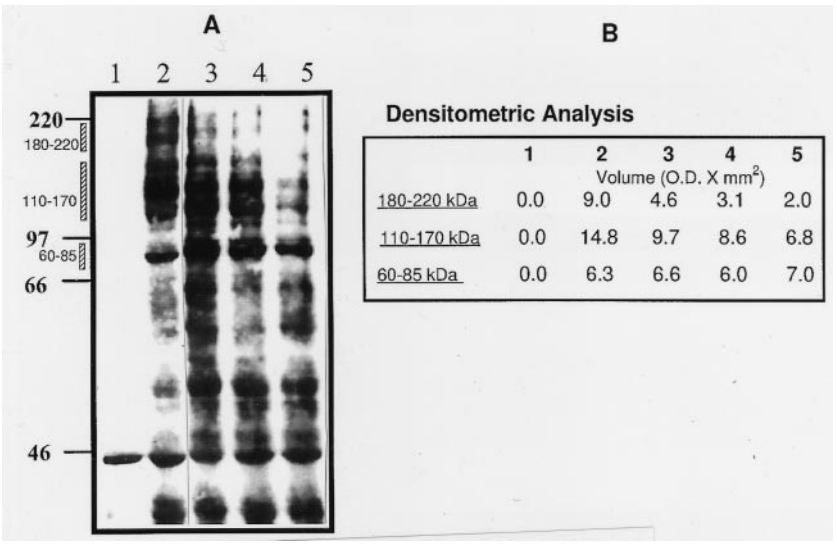

	1	2	3	4	5
		Volume (O.D. X mm²)			
180-220 kDa	0.0	9.0	4.6	3.1	2.0
110-170 kDa	0.0	14.8	9.7	8.6	6.8
60-85 kDa	0.0	6.3	6.6	6.0	7.0

FIG. 8. Effect of EGF (apical + basal) on XO + X-induced protein tyrosine phosphorylation (A). T-84 cell monolayers were exposed to XO + X at the apical and basal surfaces for 60 min. Various concentrations of EGF (apical + basal) were administered 60 min prior to XO + X. Proteins (10 μg) extracted 60 min after XO+X were subjected to western blot analysis of phosphotyrosine using HRP-conjugated anti-phosphotyrosine antibody. Lane 1: control; lane 2: XO + X; lane 3: 3 nM EGF + XO + X; lane 4: 10 nM EGF + XO + X; and lane 5: 30 nM EGF + XO + X. Bars on the left margin represent different sets of bands selected for densitometric analysis (B). This experiment was repeated with similar results two other times.

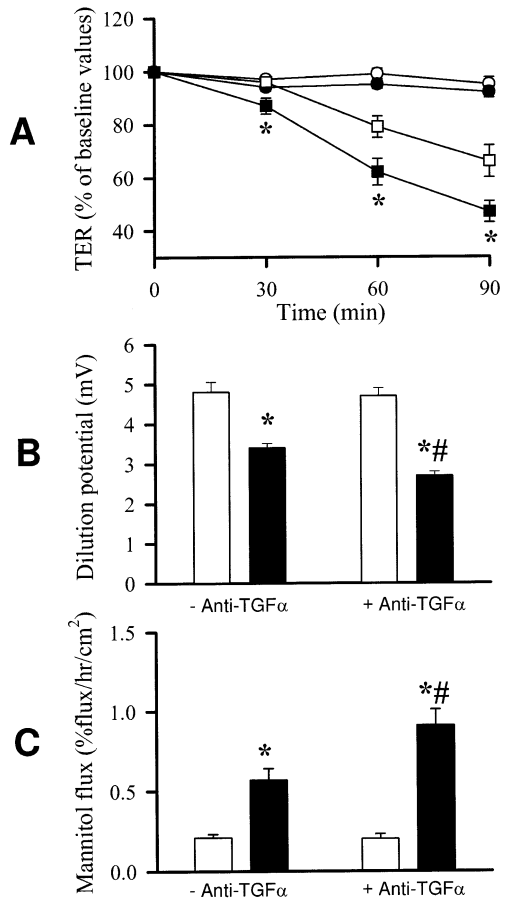

FIG. 9. (A) Effect of anti-TGF-α antibody on H_2O_2-induced decrease in TER. Caco-2 cell monolayers were treated (at both the apical and the basal surfaces) with either saline (open symbols) or 1 μg/mL of antiTGF-α antibody (closed symbols). Saline (○ and ●) or H_2O_2 (5 mM) (□ and ■) was administered to the basal surface 60 min after antibody treatment. TER measured at different times is presented as percent of baseline values. Values are means ± SEM (N = 6). Key: (*) values that were significantly ($P < 0.05$) different from corresponding time-matched values for monolayers treated with H_2O_2 alone. (B and C) Effect of anti-TGF-α antibody and pre-immune mouse IgG on H_2O_2-induced changes in dilution potential (B) and mannitol permeability (C). Caco-2 cell monolayers were treated (at both the apical and the basal surfaces) with saline or 1 μg/mL of antiTGF-α antibody. After 60 min, saline (open bars) or H_2O_2 (closed bars) was administered to the basal surface to achieve a final concentration of 5 mM. Mannitol flux was measured during 0 to 120 min of incubation with H_2O_2, while dilution potential was measured at the end of the 120-min incubation. Values are means ± SEM (N = 6). Key: (*) values that were significantly ($P < 0.05$) different from values for the corresponding saline group; and (#) values that were significantly ($P < 0.05$) different from values for the H_2O_2 without anti-TGF-α group.

[7]. EGF-mediated biologic effects are highly sensitive to tyrosine kinase inhibitors. The present study shows that genistein, a tyrosine kinase inhibitor, inhibits EGF-mediated protection from H_2O_2. The inhibition of EGF-mediated protection of epithelium by genistein indicates that this protective effect of EGF requires tyrosine kinase activity. As described, our previous study demonstrated that tyrosine kinase activity was required also for the H_2O_2-induced increase in paracellular permeability, and the H_2O_2-induced increase in paracellular permeability can be inhibited by genistein. However, the inhibition of H_2O_2-induced increase in paracellular permeability required higher concentrations of genistein (100–300 μM). A low concentration of genistein (10 μM) that inhibited EGF-mediated epithelial protection was not effective against H_2O_2-induced increase in paracellular permeability. Such a concentration-related differential inhibition of tyrosine kinases by genistein has been observed previously. The IC_{50} value of genistein for the inhibition of EGF receptor kinase [35] (~5 μM) was lower than that for the inhibition of $pp60^{c\text{-}src}$ kinase [36] (~50 μM). The mechanism by which activation of EGF receptor kinase suppresses the H_2O_2-induced protein tyrosine phosphorylation is not clear. We speculate that EGF receptor activation may lead either to activation of PTPase, which is responsible for the dephos-

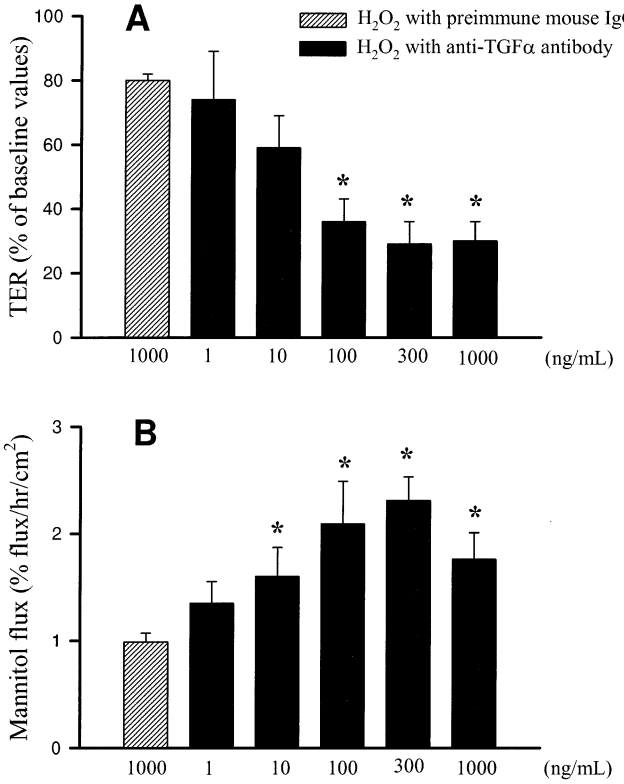

FIG. 10. Effect of different concentrations of anti-TGF-α antibody on H_2O_2-induced changes in TER (A) and mannitol permeability (B). Caco-2 cell monolayers were treated (at both the apical and the basal surfaces) with pre-immune mouse IgG (hatched bars) or with different concentrations of anti-TGF-α antibody (closed bars) 60 min prior to the administration of H_2O_2 (5 mM at the basal surface). TER measured at 90 min after H_2O_2 administration is presented as the percent of corresponding baseline values in panel A. Mannitol flux was calculated from flux measured during 0 to 150 min of incubation. Values are means ± SEM (N = 6). Key: (*) values that were significantly ($P < 0.05$) different from values for the pre-immune IgG-treated H_2O_2 group.

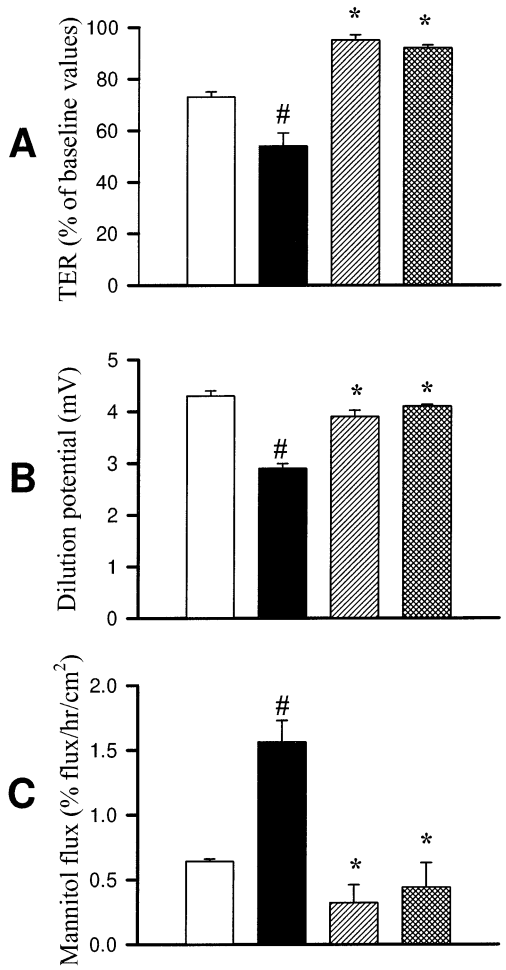

FIG. 11. Effect of anti-TGF-α antibody (100 ng/mL) on H_2O_2-induced changes in TER (A), dilution potential (B), and mannitol permeability (C): Inhibition by EGF. Caco-2 cell monolayers were treated (at both the apical and the basal surfaces) with saline (open bars), 100 ng/mL of anti-TGF-α antibody (closed bars), anti-TGF-α antibody + 30 nM EGF at the apical surface (hatched bars), or anti-TGF-α antibody + 30 nM EGF at the basal surface (cross-hatched) 30 min prior to the administration of H_2O_2 (5 mM at the basal surface). TER measured at 90 min after H_2O_2 is presented as a percent of corresponding baseline values in panel A. Mannitol flux was calculated from flux measured during 0 to 120 min of incubation. Dilution potential was measured at the end of the 120-min incubation. Values are means ± SEM (N = 6). Key: (*) values that were significantly ($P < 0.05$) different from values for the H_2O_2 group (with no treatment), and (#) values that were significantly ($P < 0.05$) different from values for the control group.

phorylation of junctional proteins, or to an inhibition of tyrosine kinases that are required to phosphorylate the key regulatory proteins. Testing this speculation, however, requires an understanding of the identity and role of specific PTPases and tyrosine kinases involved in the regulation of paracellular permeability.

Caco-2 cells have been shown previously to express the gene for TGF-α [21] and to secrete TGF-α protein [22]. TGF-α regulates proliferation of Caco-2 cells in an autocrine fashion [21]; however, the proliferative effect of TGF-α was absent in differentiated Caco-2 cells [37], although TGF-α activates MAP kinase in both undifferentiated (proliferative) and differentiated (non-proliferative) Caco-2 cells [37]. These studies suggest that TGF-α may have different functions in differentiated and undifferentiated cells. In the present study, we show that a monoclonal anti-TGF-α antibody significantly potentiated H_2O_2-induced changes in TER, dilution potential, and mannitol flux. This observation indicates that endogenous TGF-α exerts a significant protection against H_2O_2-induced epithelial injury.

In summary, this study shows that an EGF receptor-mediated mechanism inhibited H_2O_2-induced disruption of the paracellular barrier function in Caco-2 and T-84 cell monolayers. We speculate that EGF may protect the intestinal epithelium from oxidant-induced damage under physiologic and/or pathophysiologic conditions by preserving the integrity of paracellular junctional complexes.

This study was supported by a grant from the University Research Committee, Medical University of South Carolina.

References

1. Halliwell B and Cross CE, Oxygen-derived species: Their relation to human disease and environmental stress. *Environ Health Perspect* **102** (Suppl 10)**:** 5–12, 1994.
2. Harris ML, Schiller HJ, Reilly PM, Donowitz M, Grisham MB and Buckley GB, Free radicals and other reactive oxygen metabolites in inflammatory bowel disease: Cause, consequence or epiphenomenon? *Pharmacol Ther* **53:** 375–408, 1992.
3. Petrone WF, English DK, Wong K and McCord JM, Free radicals and inflammation: Superoxide-dependent activation of a neutrophil chemotactic factor in plasma. *Proc Natl Acad Sci USA* **77:** 1159–1163, 1980.
4. Vissers MCM, Day WA and Winterbourn CC, Neutrophils adherent to a nonphagocytosable surface (glomerular basement membrane) produce oxidants only at the site of attachment. *Blood* **66:** 161–166, 1985.
5. Rao RK, Baker SS, Baker RD, Gupta A and Holycross M, Oxidant-induced disruption of the intestinal epithelial barrier function: Role of protein tyrosine phosphorylation. *Am J Physiol* **36:** G812–G823, 1997.
6. Cohen S, Isolation of mouse submaxillary gland protein accelerating incisor eruption and eyelid opening in the newborn animal. *J Biol Chem* **237:** 1555–1562, 1962.
7. Carpenter G, Receptors for epidermal growth factor and other polypeptide mitogens. *Annu Rev Biochem* **56:** 881–914, 1987.
8. Konturek JW, Brzozowski T and Konturek SJ, Epidermal growth factor in protection, repair, and healing of gastroduodenal mucosa. *J Clin Gastroenterol* **13:** s88–s97, 1991.
9. Konturek SJ, Brzozowski T, Piastucki I, Dembinski A, Radecki T, Dembinska-Kiec A, Zmuda A and Gregory H, Role of mucosal prostaglandins and DNA synthesis in gastric cytoprotection by luminal epidermal growth factor. *Gut* **22:** 927–932, 1981.
10. Konturek PK, Brzozowski T, Konturek SJ and Dembinski A, Role of epidermal growth factor and sulfhydryls in stress-induced gastric lesions. *Gastroenterology* **99:** 1607–1615, 1990.
11. Konturek SJ, Brzozowski T, Konturek PK, Majka J and

Dembinski A, Role of salivary glands and epidermal growth factor (EGF) in gastric secretion and mucosal integrity in rats exposed to stress. *Regul Pept* **32:** 203–215, 1991.
12. Brzozowski T, Majka J, Garlicki J, Drozdowicz D and Konturek SJ, Role of polyamines and prostaglandins in gastroprotective action of epidermal growth factor against ethanol injury. *J Clin Gastroenterol* **13** (Suppl 1): S98–S102, 1991.
13. Itoh M, Imai S, Joh T, Kawai A, Katsumi K, Yokochi K and Takeuchi T, Protection of gastric mucosa against ethanol-induced injury by intragastric bolus administration of epidermal growth factor combined with hydroxypropylcellulose. *J Clin Gastroenterol* **14** (Suppl 1)**:** S127–S130, 1992.
14. Tepperman BL and Soper BD, Effect of epidermal growth factor on the ontogenic response of rat gastric mucosa to H^+. *Am J Physiol* **257:** G851–G859, 1989.
15. Tepperman BL, Vozzolo BL and Soper BD, Effect of maternal sialoadenectomy on ontogenic response of rat gastric mucosa to luminal H^+. *Am J Physiol* **265:** G354–G360, 1993.
16. Kirkegaard P, Olsen PS, Poulsen SS and Nexo E, Epidermal growth factor inhibits cysteamine-induced duodenal ulcers. *Gastroenterology* **87:** 103–108, 1983.
17. Ishikawa S, Cepinskas G, Specian RD, Itoh M and Kvietys PR, Epidermal growth factor attenuates jejunal mucosal injury induced by oleic acid: Role of mucus. *Am J Physiol* **267:** G1076–G1077, 1994.
18. Procaccino F, Reinshagen M, Hoffman P, Zeeh JM, Lakshmanan J, Roberts JA, Patel A, French S and Eysselin VE, Protective effect of epidermal growth factor in an experimental model of colitis in rats. *Gastroenterology* **107:** 12–19, 1994.
19. Rao R and Porreca F, Epidermal growth factor protects mouse ileal mucosa from Triton X-100-induced injury. *Eur J Pharmacol* **303:** 209–212, 1996.
20. Beaulieu J-F and Quaroni A, Clonal analysis of sucrase–isomaltase expression in the human colon adenocarcinoma Caco-2 cells. *Biochem J* **280:** 599–608, 1991.
21. Bishop WP, Lin J, Stein CA and Krieg AM, Interruption of a transforming growth factor α autocrine loop in Caco-2 cells by antisense oligodeoxynucleotides. *Gastroenterology* **109:** 1882–1889, 1995.
22. Hidalgo IJ, Raub TJ and Borchardt RT, Characterization of the human colon carcinoma cell line (Caco-2) as a model for intestinal epithelial permeability. *Gastroenterology* **96:** 736–749, 1989.
23. Peterson MD, Bement WM and Mooseker MS, An *in vitro* model for the analysis of intestinal brush border assembly. II. Changes in expression and localization of brush border proteins during cell contact-induced brush border assembly in Caco-2BBe cells. *J Cell Sci* **105:** 461–472, 1993.
24. Madara JL, Barenberg D and Carlson S, Effects of cytochalasin D on occluding junctions of intestinal absorptive cells: Further evidence that the cytoskeleton may influence paracellular permeability and junctional charge selectivity. *J Cell Biol* **102:** 2125–2136, 1986.
25. Cross HS and Quaroni A, Inhibition of sucrase–isomaltase expression by EGF in the human colon adenocarcinoma cells, Caco-2. *Am J Physiol* **261:** C1173–C1183, 1991.
26. Rao RK, Biologically active peptides in the gastrointestinal lumen. *Life Sci* **48:** 1685–1704, 1991.
27. Scheving LA, Shiurba RA, Nguyen TD and Gray GM, Epidermal growth factor receptor of the intestinal enterocyte. Localization of lateral basal but not brush border membranes. *J Biol Chem* **264:** 1735–1741, 1989.
28. Thompson JF, Vandenberg M and Stokkers PCF, Developmental regulation of epidermal growth factor receptor kinase in rat intestine. *Gastroenterology* **107:** 1278–1287, 1994.
29. Baker RD, Baker SS and LaRosa K, Polarized Caco-2 cells, Effect of reactive oxygen metabolites on enterocyte barrier function. *Dig Dis Sci* **40:** 510–518, 1995.
30. Djuric Z, Everett CK and Luongo DA, Toxicity, single-strand breaks, and 5-hydroxymethyl-2′-deoxyuridine formation in human breast epithelial cells treated with hydrogen peroxide. *Free Radic Biol Med* **14:** 541–547, 1993.
31. Kim KJ and Suh DJ, Asymmetric effects of H_2O_2 on alveolar epithelial barrier properties. *Am J Physiol* **264:** L308–L315, 1993.
32. LaCagnin LB, Bowman L, Ma JYC and Miles PR, Metabolic changes in alveolar type II cells after exposure to hydrogen peroxide. *Am J Physiol* **259:** L57–L65, 1990.
33. Takeda S, Horrobin DF, Manku M, Sim PG, Ells G and Simmons V, Lipid peroxidation in human breast cancer cells in response to γ-linolenic acid and iron. *Anticancer Res* **12:** 329–334, 1992.
34. Welsh MJ, Shasby DM and Husted RM, Oxidants increase paracellular permeability in a cultured epithelial cell line. *J Clin Invest* **76:** 1155–1168, 1985.
35. Akiyama T, Ishida J, Makagawa S, Ogawara H, Watanabe S, Itoh M, Shibuya M and Fukami I, Genistein, a specific inhibitor of tyrosine-specific protein kinases. *J Biol Chem* **262:** 5592–5595, 1987.
36. Geissler JF, Traxler P, Regehass U, Murray BJ, Roesel JL, Meyer T, McGlynn E, Storni A and Lydon MB, Thiazolidinediones. Biochemical and biologic activity of a novel class of tyrosine protein kinase inhibitors. *J Biol Chem* **265:** 22255–22261, 1990.
37. Huang F, Sauma S, Yan Z and Friedman E, Colon absorptive epithelial cells lose proliferative response to TGFα as they differentiate. *Exp Cell Res* **219:** 8–14, 1995.